

# Extended Operating Temperature XFP Optical Transceiver for 80km Reach Application up to 11.1 Gbit/s

Shinya SUZUKI\*, Shingo INOUE, Masato HINO, Yasuhiro HAMAJIMA, Kazutoshi OTSUBO and Kenji OTOBE

We have successfully developed an XFP (10 Gbit/s small form factor pluggable) optical transceiver module supporting long link distance up to 80 km at 11.1 Gbit/s, which satisfies all of the requirements by XFP multi source agreement (MSA). Power dissipation of the transceiver is less than 3.5 W under extended operating temperature ranging from -5 to +85°C, which is 20% lower than that of the conventional XFP design. Those features are considered to contribute to down-sizing and cost reduction of transmission equipment.

Keywords: XFP, LR-2, extended operating temperature, 11.1 Gbit/s, low power dissipation

## 1. Introduction

In recent years the demand for data traffic of trunk line has significantly increased and high performance transmission equipment applying higher bit-rate or WDM (wavelength division multiplexing) technologies have been introduced to the market to catch up the demand. The XFP (10 Gbit/s small form factor pluggable) is one of the most popular form factors used in 10 Gbit/s transmission equipment, which can be hot-plugged into a host board of the equipment. Most direct way to increase total data capacity is to install more host boards or to install more XFPs to one board. However, in these ways, the performance of the factor can be limited by the thermal condition, so new features like low power dissipation or extended operating temperature range are desired in order for the XFP to breakthrough the limit.

We focused on extended operating temperature up to +85°C, higher bit-rate up to 11.1 Gbit/s, and longer link distance up to 80 km, and have successfully developed XFP that complies with all features mentioned here, and that can specify power dissipation of 3.5 W.

In this paper, we report the design of the newly developed XFP that enabled the -5 to +85°C operating temperature and the 3.5 W power dissipation along with evaluation results.

## 2. Architecture

### 2-1 Specification

The appearance and main specifications of the developed XFP transceiver are shown in **Photo 1** and **Table 1**, respectively. Mechanical and electrical characteristics are fully compliant with XFP MSA<sup>(1)</sup>, and design challenge was to meet both specification of the -5 to +85°C extended operating temperature and the 3.5 W power dissipation. Optical characteristics refer to ITU-T P1L1-2D2 (equivalent to Telcordia LR-2) and 1L1-2D2F for 9.95 Gbit/s and 11.1 Gbit/s, respectively<sup>(2)</sup>. Link distance is 80 km that corre-

sponds with 0 to +1,600 ps/nm chromatic dispersion and the maximum attenuation of 22 dB. Design challenge, here, was to keep stable optical performance up to +85°C and up to 11.1 Gbit/s consistently. There is no public standard that specifies sensitivity and its dispersion penalty at 11.1 Gbit/s of bit error rate (BER) of  $10^{-12}$  with FEC disabled, so we set these targets as -23 dBm maximum and 3 dB maximum, respectively.

**Figure 1** shows basic architecture and interconnection between each functional block in the XFP transceiver. The transceiver consists of blocks of a transmitter, receiver, and control system. Following sections describe the details of the blocks.



Photo 1. XFP

### 2-2 Transmitter

The transmitter block, in the **Fig. 1**, consists of five sub-blocks: (i) TOSA (transmitter optical sub-assembly) as E/O converter, (ii) APC (automatic power control) loop to control injection current of CW-LD inside TOSA, (iii) ATC (automatic temperature control) loop to control laser temperature assembled on TEC (thermoelectric cooler) inside TOSA, (iv) LDD (laser diode driver) to drive EA (electro-absorption) modulator, and (v) Tx CDR

**Table 1.** Specification of XFP

Items		Specified values
Operation case temperature		-5°C to +85°C
Mechanical dimension		L78.0, W18.35, H8.5 mm (12.2 cm <sup>3</sup> , XFP MSA compliant)
Electrical interface		XFI (XFP MSA compliant)
Signaling speed		9.95 to 11.1 Gbit/s
Transmitter	E/O technology	EML
	Wavelength	1,530 to 1,565 nm
	Optical average power	0 to +4 dBm
	Eye mask	Compliant with Telcordia GR-253
	Dynamic extinction ratio	> 9 dB
	Jitter generation	Compliant with Telcordia GR-253
Optical Path	Media	SMF (G.652 type)
	Chromatic dispersion	0 to +1,600 ps/nm
Receiver	O/E technology	APD
	Sensitivity (@10 <sup>-12</sup> )	< -24 dBm (9.95 Gbit/s), < -23 dBm (11.1 Gbit/s)
	Dispersion penalty	< 2 dB (9.95 Gbit/s), < 3 dB (11.1 Gbit/s)
	Overload	> -7 dBm
	Jitter tolerance	Compliant with Telcordia GR-253
	Supply voltage	+3.3 V, +5 V (+/-5%)
	Power dissipation	< 3.5 W

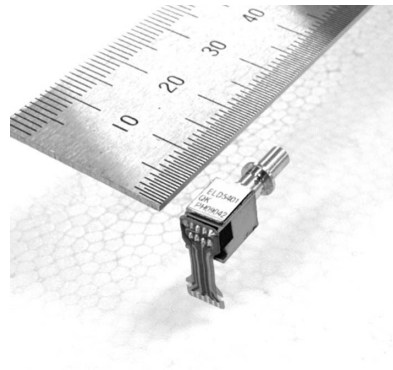


**Photo 2.** TOSA

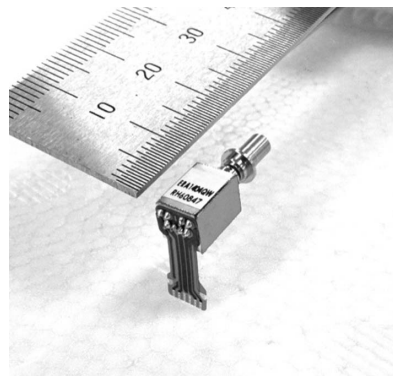


**Photo 3.** ROSA

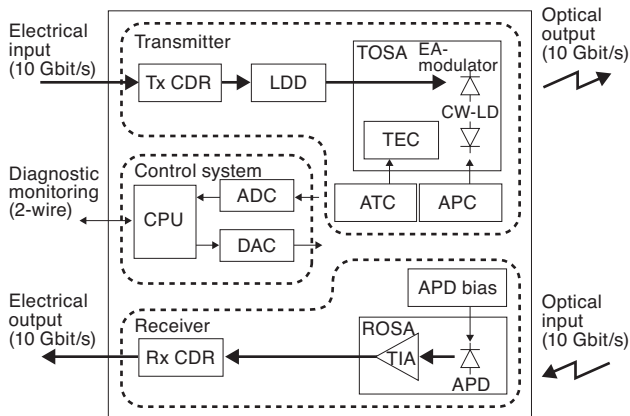


**Fig. 1.** Block diagram of XFP

(clock and data recovery) to regenerate and reshape electrical signal from host board.

**Photo 2** shows in-house TOSA assembled in the XFP, which is developed to cover 11.1 Gbit/s signaling speed over 80 km reach under the extended operating temperature. Its form factor is fully compliant with XMD-MSA (10 Gbit/s miniature device). It is electrically connected to PCB (printed circuit board) of the XFP through FPC (flexible printed circuit), and is mechanically connected to the housing of the XFP by fixing flange portion. Opti-

cal reference plane (ORP) is automatically aligned by the mechanical connection. EML (electro-absorption modulator integrated laser diode) chip<sup>(3)</sup> and TEC unit are assembled in the TOSA, and the laser chip's operating temperature is stabilized by TEC.

### 2-3 Receiver

The receiver block, in the **Fig. 1**, consists of three sub-blocks: (i) ROSA (receiver optical sub-assembly) as O/E converter, (ii) APD (Avalanche photodiode) bias control loop to control bias voltage inside ROSA, and (iii) Rx CDR to regenerate and reshape electrical signal from ROSA.

**Photo 3** shows in-house ROSA assembled in the XFP. Target application is the same as the TOSA's, and its form factor is fully compliant with XMD-MSA as well. Electrical connection, mechanical connection and optical alignment are in the same way as the TOSA's. InGaAs APD chip<sup>(4)</sup> and TIA (transimpedance amplifier) chip are assembled in the ROSA, and the APD chip's bias voltage is optimized by the APD bias control loop.

### 2-4 Control system

**Figure 2** shows the detailed architecture of control system block in the XFP transceiver. This block consists of three sub-blocks: (i) ADC (analog-digital converter) portion to monitor the operating status of XFP like case temperature etc, (ii) DAC (digital-analog converter) portion to control key parameters like EA modulation voltage etc, and (iii) CPU (central processing unit) to manage XFP's whole system including 2-wire diagnostic monitor-

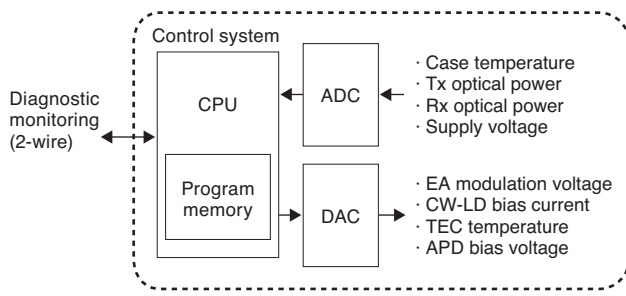


Fig. 2. Detail of XFP control system

ing interface. Through the 2-wire interface, the host board can read out the management information of the XFP, like serial ID and digital diagnostics, and can control certain functions.

### 3. Low Power Dissipation Design

#### 3-1 Conventional design

Figure 3 shows the temperature dependence of XFP power dissipation using the conventional design. Here, -5, +35 and +75°C values are based on actual measurement data, and +85°C values are estimation for the initial design. This XFP uses cooled optics, and the temperature dependence of power dissipation of the cooled optics is dominated by that of TEC and its ATC control circuit. At a higher case temperature, TEC operates as a cooler and its forward current increases. At a lower case temperature, TEC operates as a heater and its backward current increases. It has been estimated that power dissipation at +85°C is around 4 W, which is about 0.8 W larger than that of +75°C. From this estimation, it is impossible to consistently meet the -5 to +85°C and the 3.5 W operation.

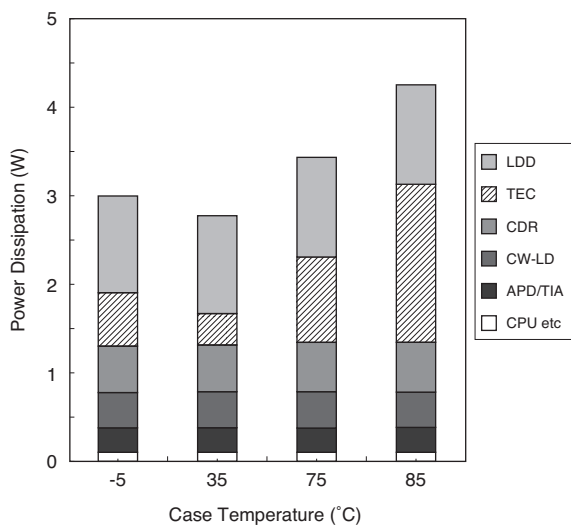


Fig. 3. Power dissipation of conventional design (estimation)

In a real operation, when TEC's required power dissipation exceeds ATC circuit's drive capability, laser chip temperature start increasing, and it causes the increase of the injection current of EML chip to compensate the drop of optical output power, and it causes the increase of thermal load on the TEC. As a result, XFP operation becomes unstable, and goes to thermal runaway mode eventually. In order to prevent this mode, there are two possible approaches; one is to reduce effective thermal load on TEC, and the other is to improve the capability of ATC drive circuit.

Besides the TEC related portion, there was still room to decrease power dissipation of the conventional design XFP. Next section describes individual approaches taken by new design.

#### 3-2 New Design

In order to achieve the design target of the -5 to +85°C operating temperature range and the 3.5 W power dissipation, following four new technologies were incorporated to the new XFP. As a consequence, almost all design has been changed.

- (1) Innovated TEC related thermal design by introducing in-house high efficiency EML chip to reduce thermal load on TEC, and by improving the capability of the ATC drive circuit.
- (2) Innovated TOSA driving circuit efficiency by changing LDD to a low voltage type, and by improving the voltage conversion efficiency of the APC circuit.
- (3) Changed CDR to a low power type.
- (4) Improved the efficiency of APD/TIA bias circuit.

Figure 4 shows the temperature dependence of XFP power dissipation using the new design. Here, -5, +35, +75 and +85°C values are estimation for this design purpose. The dominant of power dissipation is still that of TEC and its control circuit, but significant reduction of about 0.3 W at +85°C has been expected compared to the conventional design (Fig. 3). Secondary, LDD and CW-LD portions contribute to about 0.2 W reductions each. Totally, 0.8 to 0.9 W reduction has been expected.

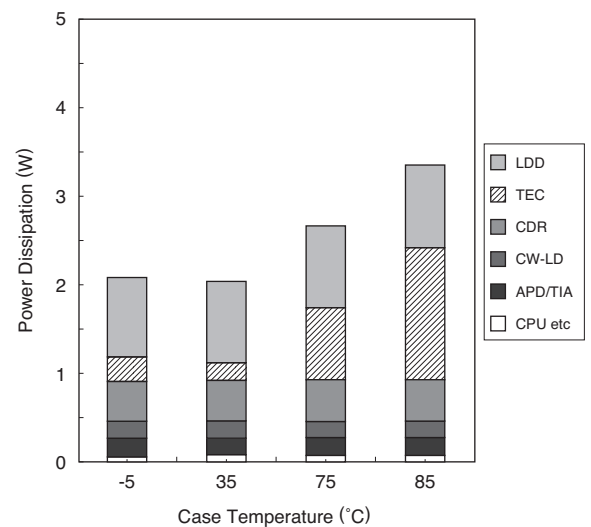
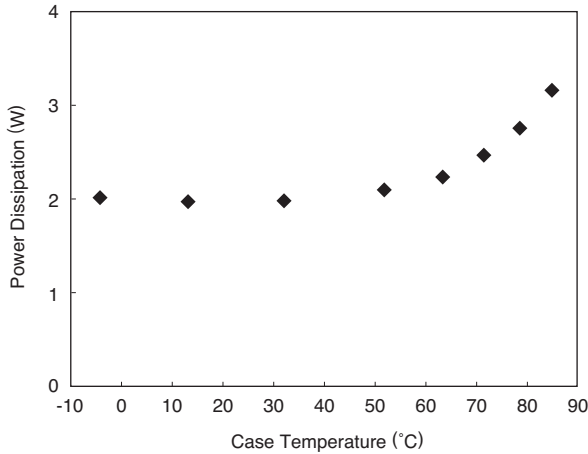


Fig. 4. Power dissipation of new design (estimation)

## 4. Evaluation Results

### 4-1 Power dissipation

**Figure 5** shows the measured temperature dependence of the power dissipation of the new design. The power dissipation is about 2.6 W and 3.2 W at +75°C and +85°C, respectively, and compliant with the target of 3.5 W, which is equivalent to 20% reduction. Note that those values are similar to the estimation.



**Fig. 5.** Power dissipation of new design (measured)

### 4-2 Optical waveform

**Figure 6** shows the transmit eye diagram before transmission and after transmission at 9.95 Gbit/s and 11.1 Gbit/s measured at +35°C. Generally, transmitter performance, including eye opening, of “before” and “after” transmission is in a trade-off relation, and the offset bias voltage applied to EA modulator is one of the most important parameters to optimize the performance. We have adequately adjusted the parameters for the product. Note that the words after transmission mean +1,600 ps/nm transmission in this paper unless otherwise described.

### 4-3 Wavelength Stability

**Figure 7** shows the measured temperature dependence of the wavelength drift of the new design. Values are normalized to that of +35°C. Stable operation within +/-25

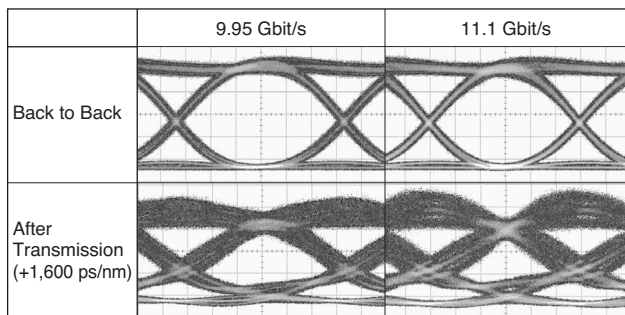


**Fig. 6.** Optical output (eye diagram)

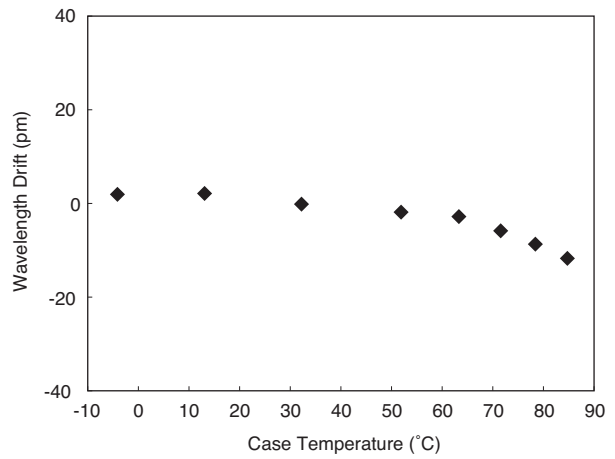


**Fig. 7.** Wavelength stability over temperature

pm precise control has been observed over temperature, and it is a promising result when we extend this design to DWDM application.

### 4-4 Receiver sensitivity

**Figure 8** shows the 11.1 Gbit/s BER (bit error rate) plots of the receiver sensitivity measured at +35°C. Regarding back to back sensitivity, there is enough margin, in comparison to the target specification of -23 dBm (see **Table 1**), and penalty free operation can be observed.

**Figure 9** shows the temperature dependence of the 11.1 Gbit/s receiver sensitivity. Both sensitivities of back to back and after transmission degrade at a higher temperature range, but still have enough margins. The dispersion penalty defined by the difference between both sensitivities also has enough margins compared to the target specification of 3 dB.

**Figure 10** shows the dispersion penalty tolerance of chromatic dispersion and signaling speed. The higher signaling speed is selected, the larger dispersion penalty is observed on the whole. In the positive chromatic dispersion

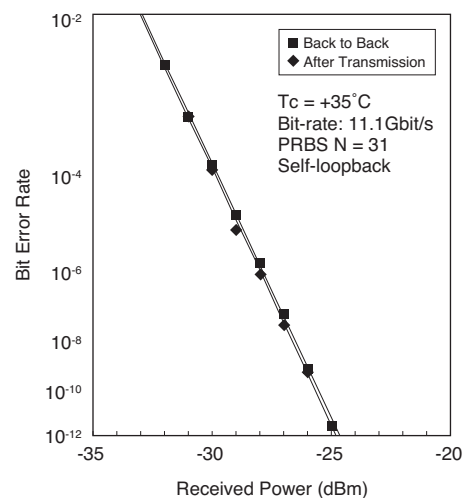


**Fig. 8.** BER characteristics

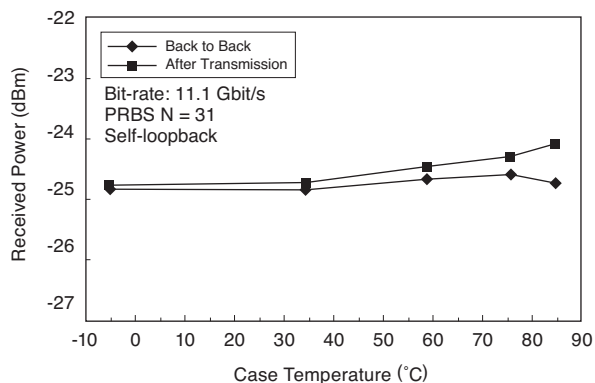


Fig. 9. Rx sensitivity temperature dependence

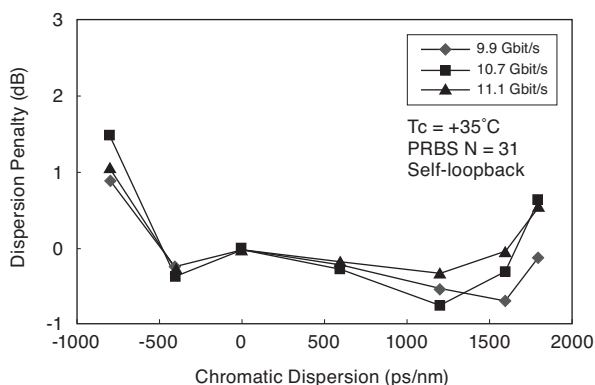


Fig. 10. Dispersion tolerance

area, the measured values go negative under +1,200 ps/nm and start increasing over +1,600 ps/nm. Negative chromatic dispersion is not required for non-DWDM application, so operating parameters have not been optimized for the negative dispersion use, but still the measurement results show less than 2 dB penalty, which holds a potential for the extended application of this design to DWDM.

#### 4-5 Jitter tolerance

Figure 11 shows the measurement result of jitter tol-

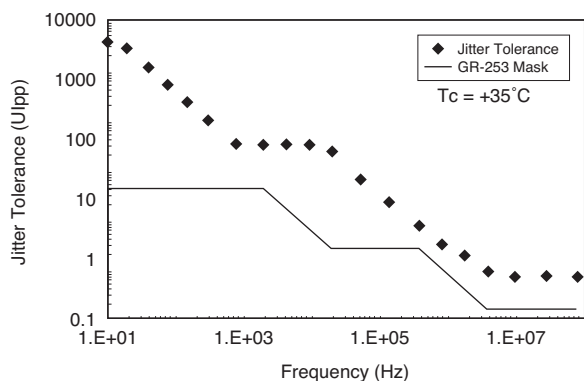


Fig. 11. Jitter tolerance

erance, and its specification limit defined by the GR-253 standard. We have confirmed that the performance is compliant with the standard.

## 5. Conclusion

We have successfully developed an XFP optical transceiver module supporting long link distance up to 80 km at 11.1 Gbit/s, and its power dissipation is less than 3.5 W under the extended operating temperature range through -5 to +85°C. In order to achieve these new features, we incorporated new technologies, such as innovative low power dissipation components and improved circuit efficiency. Those features are considered to contribute to the downsizing and cost reduction of transmission equipment.

Build a low-carbon economy is becoming a world trend. We believe that the low power dissipation and small form factor will be the key to the trend, and hope that this new development will contribute to the trend.

## References

- (1) SFF Committee, "10 Gigabit Small Form Factor Pluggable Module," INF-8077i, Rev. 4.5, 2005.
- (2) ITU-T G.959.1, "Optical Transport Network Physical Layer Interfaces," and Telcordia GR-253-CORE, "SONET Transport Systems: Common Generic Criteria."
- (3) K. Morito, R. Sahara, K. Sato, and Y. Kotaki, "Penalty-Free 10Gb/s NRZ Transmission over 100km of Standard Fiber at 1.55 $\mu$ m with a Blue-Chirp Modulator Integrated DFB Laser," IEEE Photon. Technol. Lett, vol. 8, no. 3, pp. 431-433, 1996.
- (4) Y. Kito, H. Kuwatsuka, T. Kumai, M. Makiuchi, T. Uchida, O. Wada, and M. Mikawa, "High-Speed Flip-Chip InP/InGaAs Avalanche Photodiode with Ultralow Capacitance and Large Gain-Bandwidth Products," IEEE Photon. Technol. Lett, vol. 3, no. 12, pp. 1115-1116, 1991.

## Contributors (The lead author is indicated by an asterisk (\*)).

### S. SUZUKI\*

- Assistant Manager,  
Integrated Transmission Module R&D  
Department,  
Transmission Devices R&D Laboratories

He is engaged in the research and development of the optical transceiver module for optical communications.



### S. INOUE

- Integrated Transmission Module R&D Department,  
Transmission Devices R&D Laboratories

### M. HINO

- Integrated Transmission Module R&D Department,  
Transmission Devices R&D Laboratories

Y. HAMAJIMA

- Integrated Transmission Module R&D Department,  
Transmission Devices R&D Laboratories

K. OTSUBO

- Assistant Manager,  
Integrated Transmission Module R&D Department,  
Transmission Devices R&D Laboratories

K. OTOBE

- Manager,  
Integrated Transmission Module R&D Department,  
Transmission Devices R&D Laboratories